An Amati-Bertocchi-Fubini-Stanghellini-Tonin-model description of $\pi^- p \to 2\pi^- 2\pi^+ n$ *

Jan W. Dash
Argonne National Laboratory, Argonne, Illinois 60439

S. T. Jones[†‡]
University of Alabama, University, Alabama 35486

(Received 17 January 1974)

The Amati-Bertocchi-Fubini-Stanghellini-Tonin model modified by a certain theoretically motivated $\pi\pi$-resonance off-shell behavior is applied to the 5-particle reaction $\pi^- p \to 2\pi^- 2\pi^+ n$ with *no* free parameters. The calculation is consistent with factorization of the multiperipheral model and previous phenomenology involving 3-, 4-, and 6-body exclusive data. Reasonable agreement in normalization and distributions is obtained. When this multiperipheral model is supplemented by a simple nonperipheral baryon-exchange model, the agreement is very good.

I. INTRODUCTION

In previous work, the Amati-Bertocchi-Fubini-Stanghellini-Tonin (ABFST) model[1] modified by a certain $\pi\pi$-resonance form factor $V_{\rm off}(t_{\pi 1}, t_{\pi 2})$ was presented[2] and compared with certain inclusive[3] and exclusive[4] data. The crucial feature of the modification is an enhancement of the double-off-shell momentum transfers $t_{\pi 1}, t_{\pi 2}$ at an internal vertex in the multiperipheral ABFST chain. Such enhancement, while retaining the basic peripheral nature of the model, is nevertheless strong enough to improve greatly the predictions of generated Regge intercepts in the ABFST model. Use of this modified ABFST resonance model for the single-fireball cross section[5] generates a bare Pomeron intercept $\hat{\alpha}_0 \approx 0.85$, the value used in phenomenological absorption-model calculations[6] and triple-Regge fits.[3] It is of great interest to examine the extent to which this model actually describes the inelastic cross sections. This exercise, begun in Ref. 4 for the 6-prong reaction

$$\sigma_6^+ = \sigma(\pi^+ p \to 3\pi^+ 2\pi^- p), \tag{1}$$

is extended here to the 5-particle reaction

$$\sigma_5^- = \sigma(\pi^- p \to 2\pi^- 2\pi^+ n). \tag{2}$$

The ABFST amplitude for σ_5^-, drawn in Fig. 1 and described in detail in the Appendix, contains the same $\pi\pi$ elastic amplitudes as σ_6^+, and in particular possesses a double-off-shell factor $V_{\rm off}$. We shall take the parameterization of $V_{\rm off}$ directly from our previous description of σ_6^+, and use on-shell $\pi\pi$ phase shifts to describe the $\pi\pi$ amplitudes. A single-off-shell factor $V_{\rm off}(t', m_\pi^2)$ also appears, and $V_{\rm off}$ has been constructed so that its single-off-shell behavior is roughly identical to conventional single-off-shell form factors[7] (its double-off-shell behavior is, however, much different). As mentioned in Ref. 4, our calculation of σ_6^+ is thus in agreement with factorization and previous phenomenology[8] for the 4-prong reactions

$$\begin{aligned} &\pi^+ p \to \rho^0 \Delta^{++}, \\ &p\bar{p} \to \Delta^{++}\bar{\Delta}^{--}. \end{aligned} \tag{3}$$

We shall utilize the $\pi N\bar{N}$ vertex for σ_5^- which was used in certain one-pion-exchange descriptions of the 3-body processes[8,9]

$$\begin{aligned} &\pi^- p \to \rho^0 n, \\ &pp \to \Delta^{++} n \end{aligned} \tag{4}$$

and will thus be consistent with these descriptions. The double-pion-exchange model is completely specified by factorization. *Thus our ABFST model as applied to σ_5^- has absolutely no free parameters.*

There are, needless to say, many dynamical effects which could be imagined *a priori* which are not explicitly represented in the ABFST model. We can show that some effects need not worry us, while one is more important. First, diffractive effects in our $\pi\pi$ amplitudes are not likely to be important in σ_5^- at the energies we are concerned with ($P_{\rm lab} < 20$ GeV/c), because of a lack of phase space. A quasi-two-body diffractive process such as $\pi^- p \to A_2^- N^{*+}$ is conceivable, but the data show no clear signal for either resonance. We shall have more to say about this later. Second, the pion propagators used here are elementary, but since a Reggeized pion description would involve large absorptive cuts at the small subenergies involved, the deviation from a flat effective-pion trajectory would probably not be too significant. Third, our $\pi\pi$ amplitudes are equivalent, in a dual sense, to certain Regge-exchange amplitudes (ρ and perhaps f), but certainly superior to these phenomenologically. In short, none of the above effects seem to be called for by the data, except insofar as the ABFST model approximates them. We are also

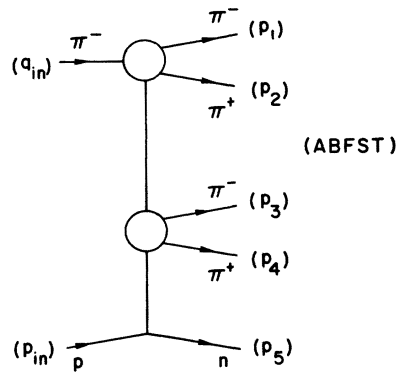

FIG. 1. ABFST multiperipheral diagram for the amplitude of $\sigma_5^- = \sigma(\pi^- p \to 2\pi^- 2\pi^+ n)$.

justified in ignoring those ABFST diagrams with $\pi^-\pi^-$ and $\pi^+\pi^+$ elastic amplitudes, as these are small.

There is, however, at least one dynamical effect which is in no theoretical sense being included, and which the ABFST model is phenomenologically unable to reproduce. This is, logically enough, a nonperipheral effect, which should be representable by some generalized u-channel baryon-exchange mechanism. In this case, the presence of Δ^- production in the data also seems to suggest this possibility, since if the Δ^- were produced as a proton fragment, double charge exchange would result. We have therefore constructed a simple baryon-exchange (BEX) model of the form

$$\sigma_{\mathrm{BEX}} = \sigma(\pi^- p \to \rho^0 \Delta^- \pi^+), \tag{5}$$

illustrated in Fig. 2 and described in the Appendix. We do not take the baryon-exchange amplitude seriously in detail, but nevertheless it appears to complement the ABFST model in those places where it is needed. These will be described in Sec. II. We have normalized the baryon-exchange cross section σ_{BEX} to the difference between the data and the ABFST predictions. An encouraging result is that σ_{BEX} then seems to fall rapidly with

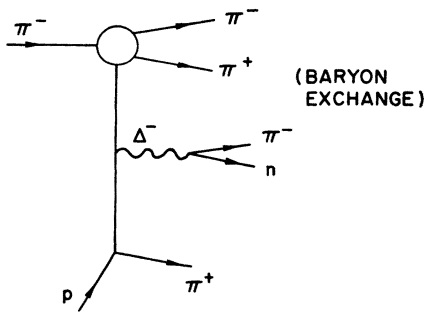

FIG. 2. Baryon-exchange (BEX) amplitude for the nonperipheral part of σ_5^-.

energy, as one would expect. Further, the longitudinal-phase-space analysis that we shall consider will reduce the BEX effect, allowing a more direct comparison between data and the ABFST model.

A final effect which may be present in the data is the production of higher-order clusters (e.g., 3π, $2\pi N$) near the threshold of σ_5^-. We shall comment on this possibility in the next section.

II. RESULTS

We have compared the model with published data at 11 GeV/c (see Refs. 10 and 11) and 16 GeV/c.[11] No higher-energy data exist. The data are presented in terms of mass and momentum plots in Ref. 10 and in longitudinal-phase-space (LPS) analysis in Ref. 11. The latter is a much better probe of the dynamics.

The ABFST-model calculations were performed using the Monte Carlo event-generating program FOWL.[12] 10^5 random, weighted events were generated at each energy, using importance sampling and cutoffs at ~ 2 GeV^2 in the momentum transfers. The resulting distributions are found to be consistent with smaller computer runs, and have been smoothed by hand in the figures. We estimate the statistical Monte Carlo errors as $\lesssim 10\%$. The baryon-exchange model was also calculated using FOWL (with somewhat poorer statistics), and as mentioned before the distributions for the two models were added together, neglecting possible interference terms. Crossed graphs were included, however, in the ABFST calculation.

We first consider the results for the normalization of the ABFST-model prediction for σ_5^-, shown in Fig. 3. It is seen that the agreement gets better at higher energies, an effect found in our analysis of σ_6^+ (Ref. 4) and in the analysis[13,8] of all 4-prong events of the type

$$\pi^+ p \to 2\pi^+ \pi^- p. \tag{6}$$

It is possible that one is seeing here the effect of higher-order clusters not included in our model, which are present in events above the average multiplicity at a given energy, and which therefore affect the threshold behavior of a given σ_n. It is known that the ABFST model generally yields a multiplicity $\langle n \rangle$ which is too low,[2] perhaps reflecting the need for clusters near threshold. We shall assume that for $P_{\mathrm{lab}} \geq 11$ GeV/c such effects have become small in σ_5^-, since at these energies $\langle n \rangle \gtrsim 5$.

At 11 GeV/c, the ABFST model yields about $\frac{2}{3}$ of the measured value of σ_5^-. We attribute the remainder to baryon exchange, as mentioned before. That this is reasonable is attested to by the fact that this is roughly the proportion of nonperipheral

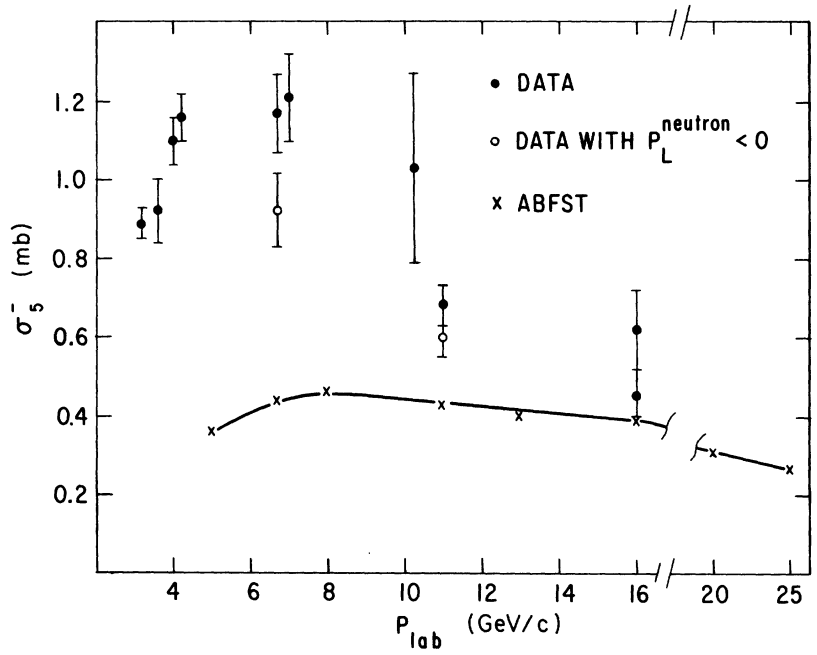

FIG. 3. Energy dependence of σ_5^- and ABFST-model prediction.

neutrons [Fig. 4(a)], Δ^- events [Fig. 7(b)], and high-4π-mass events [Fig. 8(c)], all effects which one could reasonably associate with baryon exchange. At 16 GeV/c, the baryon-exchange cross section has decreased significantly, which is consistent. At lower energies, it may well be that, in addition to baryon exchange, other effects rapidly decreasing in s contribute. We note in passing that the threshold discrepancy between the ABFST model and the observed cross section is rather larger for σ_5 than for σ_6, and that the experimental σ_5 bears a stronger resemblance to 4-particle cross sections than to 6-particle ones. Our analysis indicates, however, that the major "low-energy" dynamical mechanism for $P_{lab} \gtrsim 11$ GeV/c is baryon exchange.

We turn now to the distributions at 11 GeV/c. These are presented in Figs. 4–8. Three curves are shown. These are, respectively, dotted (ABFST), dashed (baryon exchange), and solid (ABFST + baryon exchange). The ABFST contribution alone is seen to provide qualitative agreement with all the distributions, though some discrepancies are clear. These are mainly connected with the absence of forward neutron events, Δ^- events, and high-3π- and high-4π-mass events. As we have said, these are all effects which are *a priori* ascribable to baryon exchange, and our calculation bears this out. The total of the peripheral ABFST and nonperipheral BEX models is in good agreement with all distributions. Some detailed effects,

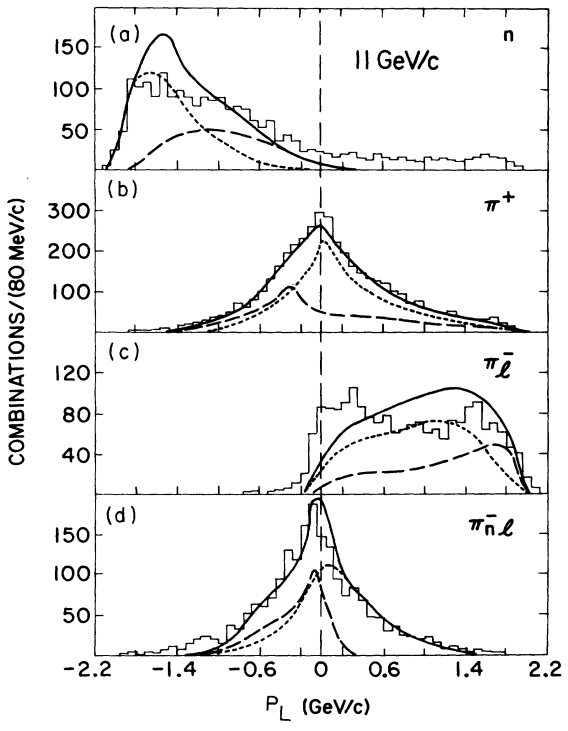

FIG. 4. Longitudinal momentum distributions at 11 GeV/c: (a) n, (b) π^+, (c) π_l^-, and (d) π_{nl}^-. π_l^- is that π^- with the smaller momentum transfer from the incident π^-; π_{nl}^- is the other π^-. The dotted, dashed, and solid lines in Figs. 4–8 correspond respectively to the ABFST, BEX, and (ABFST + BEX) models.

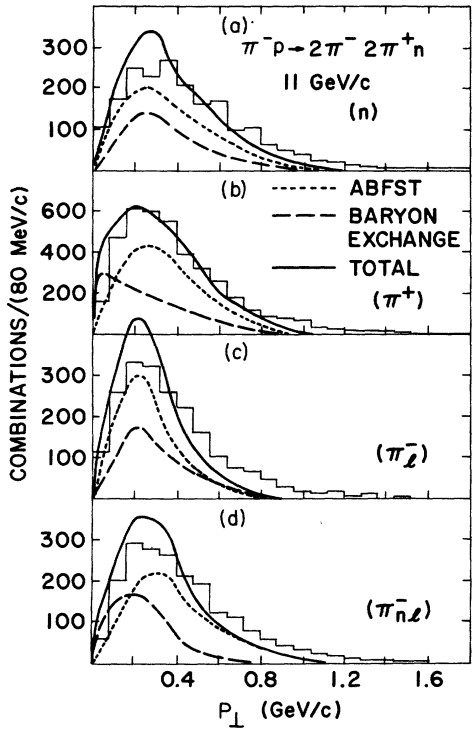

FIG. 5. Transverse momentum distributions at 11 GeV/c: (a) n, (b) π^+, (c) π^-_l, and (d) π^-_{nl}. Dotted, dashed, and solid lines as in Fig. 4.

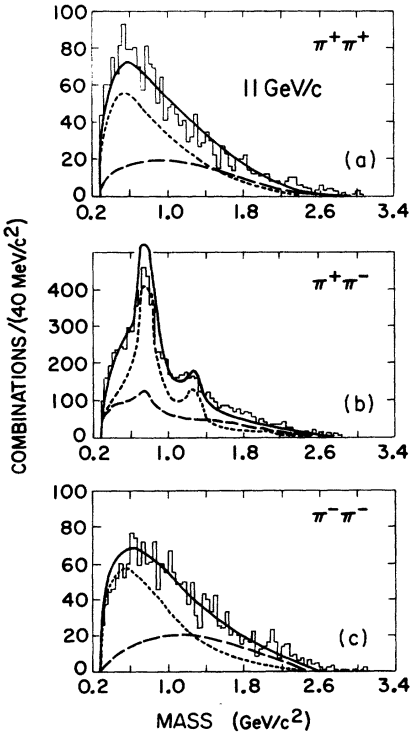

FIG. 6. $\pi\pi$ mass plots at 11 GeV/c: (a) $\pi^+\pi^+$, (b) $\pi^+\pi^-$, and (c) $\pi^-\pi^-$. Dotted, dashed, and solid lines as in Fig. 4.

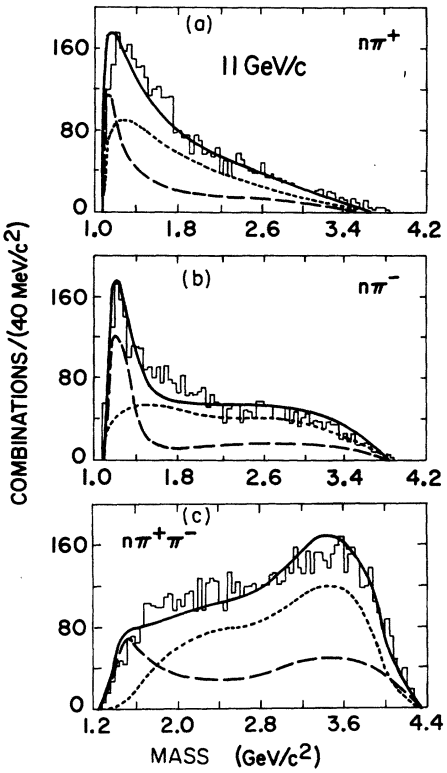

FIG. 7. πn and $\pi\pi n$ mass plots at 11 GeV/c: (a) $n\pi^+$, (b) $n\pi^-$, and (c) $n\pi^+\pi^-$. Dotted, dashed, and solid lines as in Fig. 4.

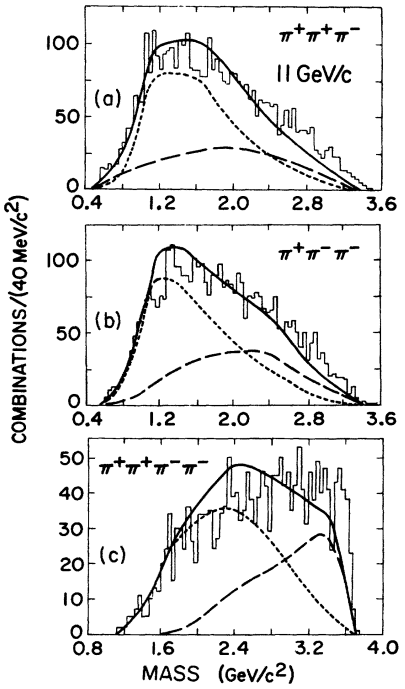

FIG. 8. 3π and 4π mass plots at 11 GeV/c: (a) $\pi^+\pi^+\pi^-$, (b) $\pi^+\pi^-\pi^-$, and (c) $\pi^+\pi^+\pi^-\pi^-$. Dotted, dashed, and solid lines as in Fig. 4.

like the magnitude of the $\pi^+\pi^-$ mass distributions near the ρ and f^0, are also improved. The longitudinal-momentum distribution of the leading π^-, defined as that one with the smaller value of $-(q_{\text{in}} - p_{\pi^-})^2$, is improved somewhat. One detail that is still not satisfactory is the small proportion of very highly nonperipheral neutrons which are still not explained. These could reasonably be attributed, e.g., to a double-baryon-exchange process, but we shall not examine this explicitly.

The preceding analysis of the 11-GeV/c data gives us some confidence that we have at least a qualitative understanding of what is going on. We turn next to the longitudinal-phase-space (LPS) analysis, which provides more stringent tests of the model. Although at infinite energy decomposition of the phase space into LPS regions readily isolates some dynamical mechanisms, we shall see that at these intermediate energies such statements can be misleading, as our ABFST model works reasonably well.

Kittel *et al.*[11] have presented weighted LPS plots for σ_5^- at 11 and 16 GeV/c. They weight each event by the "longitudinal-phase-space factor" w/s,

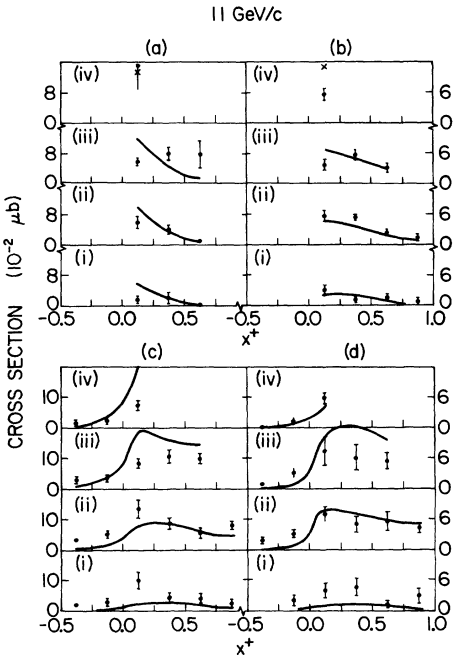

FIG. 9. LPS plots at 11 GeV/c. The variables are described in the text. Theoretical predictions are represented by the smooth curve, or by X when only one bin is occupied. Bins are defined as follows: (a) $0.25 \le x_1^+ < 0.5$, (b) $0.0 \le x_1^+ < 0.25$, (c) $-0.25 \le x_1^+ < 0.0$, (d) $-0.5 \le x_1^+ < -0.25$; (i) $-0.5 \le x_s^- < -0.25$, (ii) $-0.25 \le x_s^- < 0.0$, (iii) $0.0 \le x_s^- < 0.25$, (iv) $0.25 \le x_s^- < 0.5$. The curve is that predicted by the ABFST model without the BEX contribution and is normalized to the data. Normalizations are given in Table I.

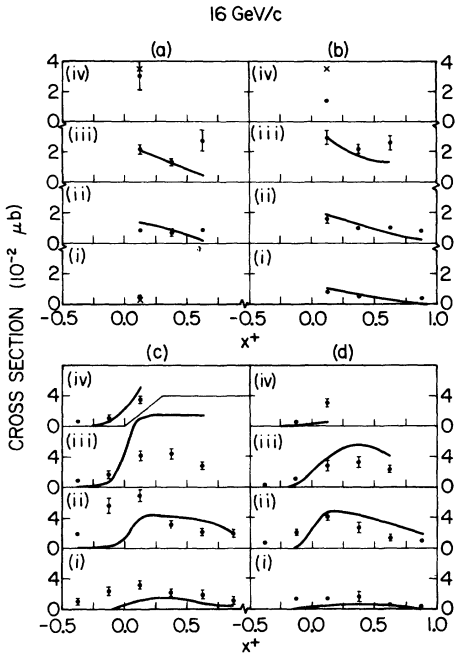

FIG. 10. LPS plots at 16 GeV/c. Notation and binning are as in Fig. 9.

where $s = (q_{\text{in}} + p_{\text{in}})^2$, and

$$w = \left[\sum_{i=1}^{N} (x_i^2 E_i^{-1})\right]\left[\tfrac{1}{2}\sum_{i=1}^{N} |(p_{\parallel})_i|\right]^{3-N}\left(\prod_{i=1}^{N} E_i\right). \tag{7}$$

Here, E_i and $p_{\parallel i}$ are the energy and longitudinal c.m. momentum, respectively, of the ith particle. N is the multiplicity, $N=5$, and x_i is called the reduced longitudinal momentum:

$$x_i = \frac{2p_{\parallel i}}{\sum_{j=1}^{N} |p_{\parallel j}|}\ . \tag{8}$$

When the events are weighted by w/s, kinematic effects of phase space are removed to some extent at least, and distributions in x and $p_\perp$ presumably reflect primarily the behavior of the square of the matrix element—i.e., the dynamics.

It is a simple manner to duplicate this analysis with our Monte Carlo events. The results are presented in terms of the weighted contribution to bins in x space, and are shown in Figs. 9 and 10. Here, x_s^- is the x for the slower π^- ($x_s^- < x_f^-$). x^+ refers to the faster π^+ when $x_f^+ > 0 > x_s^+$, and to a random selection of (x_f^+, x_s^+) when both π^+'s are in the same hemisphere. x_1^+ is the other π^+. The events are divided into bins according to values of x_s^-, x^+, and x_1^+, as shown in the figures. Only those events with $x_f^- > 0 > x_n$ are included. Note that this eliminates some fraction of the troublesome baryon-exchange events.

TABLE I. Normalizations of the LPS segments for the model and the data.

		Contents (μb)			
	LPS segment:	a	b	c	d
11 GeV/c	Experiment	0.52	0.41	1.13	0.71
	ABFST	0.19	0.38	0.76	0.32
	BEX[a]	...	...	0.36	0.35
16 GeV/c	Experiment	0.13	0.15	0.52	0.30
	ABFST	0.18	0.23	0.50	0.17
	BEX[a]	...	...	0.12	0.12

[a] BEX normalization assumes that *total* BEX contribution to σ_5^- is 0.25 mb at 11 GeV/c and 0.10 mb at 16 GeV/c.

The theoretical curves in Figs. 9 and 10 have been normalized to the data [separately for each graph (a)–(d) in each figure] in order to compare qualitative behaviors. The actual normalizations are given in Table I, and are found to agree adequately. The baryon-exchange contributions, from the model discussed above, are given in the table, but are *not* included in the figures.

At 11 GeV/c, the model and data are seen to agree well, with only a few qualitative discrepancies. In general, it is fair to say that the data tend to vary somewhat less rapidly with x^+ than does the model. The same is true at 16 GeV/c, where the data are statistically more accurate. We see here (Fig. 10) a generally adequate agreement, with the primary discrepancies in Fig. 10(c), where the data have large contributions at $x^+ < 0$, while the model has virtually none. The baryon-exchange model does contribute to this region, but not enough to completely explain the discrepancy. In addition, segment (iii) of Fig. 10(c) is already oversubscribed by the model. The experimental peak in segment (ii) of Fig. 10(c), which is not adequately explained by baryon exchange, may be partly due to single diffraction of the type

$$\pi^- p \to \pi^-(\pi^-\pi^+\pi^+ n),$$

as suggested in Ref. 11. With these exceptions, the ABFST model seems to do a good job of describing the LPS analysis.

Finally, we show in Fig. 11 the $(\pi^-\pi^-\pi^+)$ and $(\pi^+ n)$ effective mass distributions in LPS sector 5 at 16 GeV/c, defined by the c.m. longitudinal momentum separation

$$\pi^- p \to (\pi^-\pi^-\pi^+)_{\text{forward}}\,(\pi^+ n)_{\text{backward}}\,.$$

The agreement of the data and the ABFST model is very good. At high energies, sector 5 can reasonably be ascribed to a diffractive process. Our calculation shows that naive application of LPS cuts to intermediate energies can be seriously misleading, since this "diffractive" region is well described by our resonance multiperipheral model. In particular, the normalization of this sector is reasonable, being given by 0.085 mb in the model, as compared to 0.10 mb experimentally. Note that the peak in segment (iii) of Fig. 10(c), referred to above, is contained in sector 5. The large contribution from the ABFST model is thus evidence against a double-diffraction interpretation of the major portion of events in sector 5 at these energies.

III. CONCLUSIONS AND THEORETICAL COMMENTS

We have shown that the ABFST model, with suitable off-shell modifications, is capable of describing the reaction $\pi^- p \to 2\pi^- 2\pi^+ n$ with at least qualitative agreement of normalizations and distributions at 11 and 16 GeV/c. This was done with no free parameters, all parameters having been determined by previous analysis of 3-, 4-, and 6-body reactions. The smaller nonperipheral part of the cross section not described by the ABFST model was adequately described by a simple baryon-exchange model.

The theoretical motivation for consideration of the resonance ABFST multiperipheral model at

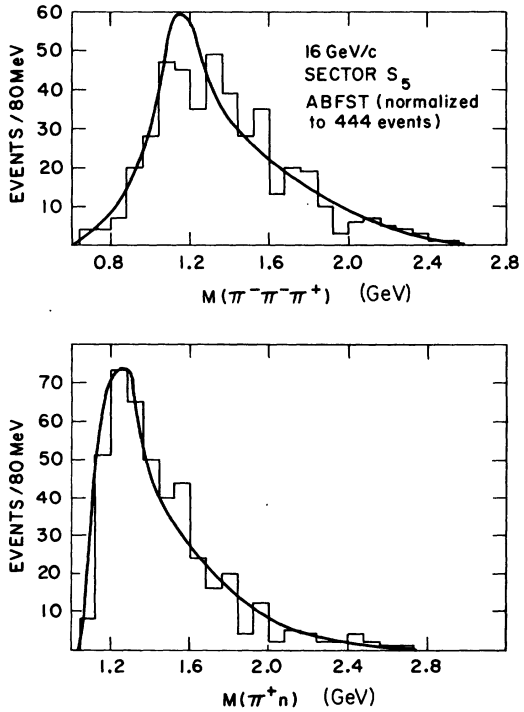

FIG. 11. Mass plots in LPS sector 5 at 16 GeV/c (defined in text): (a) $(\pi^-\pi^-\pi^+)_f$, (b) $(\pi^+ n)_b$. Only the contribution of the ABFST model is included; the normalization is given in the text.

these intermediate energies lies partially in the attempt to describe the single-fireball cross section[5] by the resonance ABFST model. This has implications in a wider sense when unitarity is utilized at intermediate energies to build up the bare Pomeron.[5] Substantial phenomenology utilizing the bare Pomeron is presently being carried out,[3,6,14] and the calculation performed here can be regarded as a consistent part of this phenomenology.

ACKNOWLEDGMENTS

S. T. Jones wishes to thank Argonne National Laboratory, where this work was begun, for its hospitality, and the Argonne Center for Educational Affairs for financial support.

APPENDIX

We present here the explicit formulas used in the calculation. The cross section for the process $\pi^- p \to 2\pi^+ 2\pi^- n$, in the ABFST model, is

$$\sigma_5^-(s) = \frac{(2\pi)^{-11}}{2!2!2\lambda^{1/2}(s, m_\pi^2, m_p^2)} \times \int \prod_{i=1}^{5} \frac{d^3p_i}{2E_i} \delta^4(q_{\text{in}} + p_{\text{in}} - \sum_{i=1}^{5} p_i) \times \tfrac{1}{2} \sum_{s_i s_f} |M^{s_i s_f}|^2 , \tag{A1}$$

where $M^{s_i s_f}$ is the symmetrized $2 \to 5$ amplitude for initial (final) nucleon spin s_i (s_f). It will be written as the sum over the four permutations:

$$M^{s_i s_f} = \sum_{j=1}^{4} M_j^{s_i s_f} . \tag{A2}$$

We define the standard permutation $j=1$ corresponding to Fig. 1, where the momenta of $(\pi^-\pi^+)(\pi^-\pi^+)(n)$ are $(p_1 p_2)(p_3 p_4)(p_5)$. For this permutation,

$$M_{j=1}^{s_i s_f} = M_{\pi\pi}(s_{12}, t_{12}; m_\pi^2, t_{23}) P(t_{23}) \times M_{\pi\pi}(s_{34}, t_{34}; t_{23}, t_{45}) P(t_{45}) M_{\pi p}^{s_i s_f}(t_{45}) \equiv \beta_{j=1} M_{\pi p}^{s_i s_f}(t_{45}) . \tag{A3}$$

Here $s_{ij} = (p_i + p_j)^2$ and $t_{ij} = (q_{\text{in}} - \sum_{k=1}^{i} p_k)^2$, where q_{in} is the incoming pion momentum. $M_{\pi\pi}(s, t; u_1, u_2)$ is the off-shell elastic $\pi^+\pi^-$ amplitude for initial particles of mass squared u_1 and u_2. The pion propagator is

$$P(t) = (t - m_\pi^2)^{-1} . \tag{A4}$$

The off-shell $\pi^- p$ Born term has the initial pion at a mass-squared of $t_{45} \equiv t_{pn}$. It is given by

$$M_{\pi p}^{s_i s_f} = \sqrt{2}\, G \bar{u}^{s_f}(p_5) \gamma_5 u^{s_i}(p_{\text{in}}) \Gamma(t_{pn}) , \tag{A5}$$

where $\Gamma(t_{pn})$ is a form factor (to be chosen later), $G^2/4\pi \approx 14.5$, and our projection operator is $(\not{p} + m)$. We have then

$$\tfrac{1}{2} \sum_{s_i s_f} |M^{s_i s_f}|^2 = \sum_{l,j=1}^{4} \beta_l \beta_j^* (\sqrt{2}\, G)^2 (-t_{pn}) \Gamma^2(t_{pn}) , \tag{A6}$$

where β_l is the meson part of $M^{s_i s_f}$ for the lth permutation.

As explained in Ref. 4, we may simplify the double sum above by a formal change of variables which is satisfied to within a statistical error on the computer. The double sum collapses, and we obtain finally

$$\sigma_5^-(s) = \frac{(2\pi)^{-11} (\sqrt{2}\, G)^2}{2\lambda^{1/2}(s, m_\pi^2, m_p^2)} \times \int \prod_{i=1}^{5} \frac{d^3p_i}{2E_i} \delta^4\Big(q_{\text{in}} + p_{\text{in}} - \sum_{i=1}^{5} p_i\Big) \times \mathrm{Re}\Big(\sum_{j=1}^{4} \beta_1 \beta_j^*\Big) (-t_{pn}) \Gamma^2(t_{pn}) . \tag{A7}$$

In the limit of infinite computer statistics, we may remove the real-part operation.

We parametrize $M_{\pi\pi}$ by its partial-wave expansion

$$M_{\pi\pi}(s, t; u_1, u_2) = \frac{16\pi s}{\lambda^{1/2}(s, m_\pi^2, m_\pi^2)} V_{\text{off}}(u_1, u_2) \times \sum_{I,l} (2l+1) C_l^I P_l(\cos\theta_{\text{off}}) \times e^{i\delta_l^I} \sin\delta_l^I , \tag{A8}$$

where $C_{2l}^0 = \frac{2}{3}$, $C_{2l}^2 = \frac{1}{3}$, and $C_{2l+1}^1 = 1$, the others vanishing. $\cos\theta_{\text{off}}$ is the cosine of the appropriate off-shell scattering angle, and our off-shell vertex $V_{\text{off}}(u_1, u_2)$, common to all partial waves, is

$$V_{\text{off}}(u_1, u_2) = \Big(1 - \frac{\tilde{u}_1}{\lambda} - \frac{\tilde{u}_2}{\lambda} + \frac{\tilde{u}_1 \tilde{u}_2}{\xi}\Big) e^{b(\tilde{u}_1 + \tilde{u}_2)} , \tag{A9}$$

where $\tilde{u} = u - m_\pi^2$. The values of the parameters used are

$$\lambda = 1.2 \text{ GeV}^2 , \quad b = 0.6 \text{ GeV}^{-2} , \quad \xi = 0.15 \text{ GeV}^4 . \tag{A10}$$

These parameters were taken from our previous analysis of the reaction $\pi^+ p \to 3\pi^+ 2\pi^- p$ in Ref. 4.

The partial-wave summation was performed using the on-shell s-, p-, and d-wave phase shifts which were assumed elastic, and the integrals were cut off for $\pi\pi$ subenergies above 1.5 GeV. These approximations are reasonable for σ_5^- at the energies considered here.

Our form factor $\Gamma(t_{pn})$ for the $pn\pi^-$ vertex was chosen conventionally for convenience. It is given by

$$\Gamma^2(t_{pn}) = \frac{1+R_n^2 q_n^2}{1+R_n^2 q_{nt}^2}, \tag{A11}$$

where $\Gamma(m_\pi^2) = 1$, and

$$\begin{aligned} q_n &= \lambda^{1/2}(m_\pi^2, m_N^2, m_N^2)/2m_N, \\ q_{nt} &= \lambda^{1/2}(t_{pn}, m_N^2, m_N^2)/2m_N. \end{aligned} \tag{A12}$$

We used $R_n = 2.66\ \mathrm{GeV}^{-1}$, as in Ref. 9. Wolf finds $R_n = 2.86\ \mathrm{GeV}^{-1}$.

The baryon-exchange model used in part of our calculation is represented by the diagram of Fig. 2. We neglected nucleon spin and did not symmetrize the amplitude. The amplitude is then

$$\begin{aligned} M_{\mathrm{BEX}} = g_B M_{\pi\pi}(s_{12}, t_{12}; m_\pi^2, t_{23}) P(t_{23}) \\ \times M^{\Delta}_{\pi N}(s_{34}, t_{34}) P_N(t_{45}). \end{aligned} \tag{A13}$$

Here $M_{\pi\pi}$ and $P(t)$ are the same $\pi\pi$ amplitude and pion propagator as described above. $P_N(t)$ is a phenomenological nucleon propagator,

$$P_N(t) = e^{2t}/(t - m_N^2). \tag{A14}$$

$M^{\Delta}_{\pi N}$ is a Breit-Wigner form with constant width, representing $\Delta^-(1236)$ production, with a decay distribution of

$$\frac{d\sigma}{d\Omega} \propto (1 + 3\cos^2\theta);$$

that is,

$$M^{\Delta}_{\pi N}(s,t) \propto \frac{1}{\sqrt{s} - m_\Delta + i\frac{1}{2}\Gamma_\Delta} (1 + 3\cos^2\theta)^{1/2}. \tag{A15}$$

For simplicity, no theoretical attempt was made to normalize the baryon-exchange amplitude, nor were form factors used in $M^{\Delta}_{\pi N}(s,t)$. The exponential coefficient in $P_N(t)$ was arbitrarily set at $2\ \mathrm{GeV}^{-2}$ to ensure peripherality of the π^+, and no attempt was made to optimize this parameter.

We have also calculated the results of a multi-Regge meson plus baryon-exchange model. Results substantially similar to the above baryon-exchange model were obtained, except that the magnitude of Δ production was insufficient.

---

*Part of this work performed under the auspices of the U. S. Atomic Energy Commission.
†Research supported in part by the Research Corporation.
‡Summer visitor at Argonne National Lab.

[1]D. Amati, A. Stanghellini, and S. Fubini, Nuovo Cimento 26, 896 (1962); L. Bertocchi, S. Fubini, and M. Tonin, *ibid.* 25, 626 (1962).
[2]J. Dash, G. Parry, and M. Grisaru, Nucl. Phys. B53, 91 (1973).
[3]J. W. Dash, Phys. Rev. D 9, 200 (1974).
[4]J. Dash, J. Huskins, and S. T. Jones, Phys. Rev. D 9, 1404 (1974).
[5]G. F. Chew, LBL Report No. LBL 2174, 1973 (unpublished).
[6]N. F. Bali and J. Dash, ANL Reports Nos. ANL/HEP 7370, 1974 (unpublished) and ANL/HEP 7372, 1974 (unpublished).
[7]J. Benecke and H. P. Dürr, Nuovo Cimento 56, 269 (1968).
[8]G. Wolf, Phys. Rev. 182, 1538 (1969).
[9]E. Colton and P. Schlein, in *Proceedings of the Conference on $\pi\pi$ and $K\pi$ Interactions, Argonne National Laboratory, 1969,* edited by F. Loeffler and E. B. Malamud (Argonne National Laboratory, Argonne, Ill., 1969).
[10]C. Caso *et al.*, Nuovo Cimento 66A, 11 (1970).
[11]W. Kittel, S. Ratti, and L. Van Hove, Nucl. Phys. B30, 333 (1971).
[12]F. James, Institut de Physique Nucléaire, Paris, report, 1966 (unpublished). Users should be aware that the random-number generator of this version must be put into double precision on certain computers.
[13]W. Kittel, CERN Report No. 73-10, 1973 (unpublished).
[14]J. W. Dash, Phys. Lett. 49B, 81 (1974).